

Investigating the Impact of Cancer-Associated PARP1 Mutations on Enzyme Function

Aryan Mangla

Dr. Soo Hyun Yang

The Biobricks for Molecular Machines FRI Stream

College of Natural Sciences

University of Texas at Austin

12/16/24

Introduction

Cellular DNA faces a constant threat of damage, and eukaryotic cells have developed various mechanisms to combat these threats, including DNA damage detection, signaling, and repair. Among these mechanisms, the enzyme Poly(ADP-ribose) polymerase 1 (PARP1) plays a pivotal role in catalyzing the addition of Poly(ADP-ribose) chains to target proteins, otherwise known as PARylation.¹ The activity of PARP1 is tightly regulated within cells, as both insufficient and excessive activity can have detrimental effects. Inactive PARP1 results in defective DNA repair, increased mutations, and potential cancer predisposition, while hyperactive PARP1 triggers cellular energy depletion and oxidative stress through NAD⁺/ATP depletion, potentially leading to tissue damage and neurodegenerative diseases.^{1,2,3}

While the fundamental mechanisms of PARP1 activation and its role in DNA repair are well-established, significant knowledge gaps remain in our understanding of how cancer-associated mutations affect PARP1 function. Despite current literature focusing on PARP1's wild-type activity and its inhibition in cancer therapy, little is known about how cancer-specific mutations might alter its enzymatic function and subsequent cellular responses. A comprehensive meta-analysis of cancer genomics databases has identified over 30 distinct PARP1 mutations across various cancer types, yet their functional implications remain largely unexplored.⁴ Recent studies have revealed critical regulatory domains within PARP1, suggesting that mutations in these regions could significantly impact enzyme function and its downstream cellular processes.⁵ However, the field needs to translate these structural insights into clearly understanding how specific cancer-associated PARP1 mutations disrupt its normal function and potentially contribute to oncogenesis. Addressing this knowledge gap could provide valuable mechanistic insights and identify new therapeutic targets for PARP1 dysfunction in cancer.³

Our study aims to address these specific knowledge gaps by examining the impact of cancer-associated PARP1 mutations on its enzymatic activity and PARylation function. We hypothesize that these mutations may alter the PARylation activity of PARP1, potentially leading to increased cellular toxicity through disruption of normal DNA repair processes and energy metabolism. To test this hypothesis, we will create PARP1 mutations via site-directed mutagenesis and employ three distinct pBAD-based bacterial expression vectors (pBB vectors) optimized for protein expression in *Escherichia coli* BL21(DE3) codon plus cells, a strain engineered to minimize protein degradation and maximize recombinant protein yield. After expressing and purifying recombinant PARP1 mutant proteins in *E. coli* BL21(DE3) codon plus cells using a combination of nickel-affinity and ion-exchange chromatography, we will conduct in vitro PARylation assays to examine how these mutations affect PARP1's enzymatic activity.

This research is significant because it has the potential to elucidate the role of PARP1 mutations in cancer pathogenesis. By examining how cancer-associated PARP1 mutations affect enzymatic activity, our study aims to clarify how these mutations may alter PARP1 function, potentially leading to disruptions in DNA repair and cellular energy balance. This targeted

understanding could provide foundational insights that connect PARP1 mutation effects directly to mechanisms of cellular dysfunction, aligning with our research purpose. Ultimately, these findings may support the broader field by informing downstream research on the role of PARP1 in oncogenesis and guiding the development of more targeted cancer therapies and management strategies for PARP1-related cellular dysfunction across various diseases.

Procedure

Expression Vectors and Primer Preparation

This study utilized three distinct *E. coli* expression vectors containing the PARP1 gene. The vectors include pBB204 containing GST-PARP1 in pGEX6-c1 (AmpR), pBB205 containing his-flag-mCherry-PARP1 in pET28 (KanR), and pBB206 containing his-SMT-HA-PARP1 in pET28 (KanR). To prepare working solutions, primers at a concentration of 1.25 µg/µL were diluted 10-fold by combining 1 µL of stock primer with 9 µL of sterile dH₂O to achieve a final concentration of 10 µM.

Site-directed mutagenesis of PARP1 D229V and Agarose Gel Electrophoresis

The PCR reaction mixture was prepared in a total volume of 25 µL. The reaction contained 12.5 µL of 2X HiFi PCR Master Mix (NEB), 1 µL of forward primer PARP45: CTAAAAAAAGAAAAAgtcAAGGATAGTAAGC and reverse primer PARP46: GCTTACTATCCTTgacTTTTCTTTTAG (125 ng/µL), 1 µL of template DNA (either pBB204, pBB205, or pBB206), 0.7 µL of DMSO, and 8.8 µL of sterile dH₂O. The PCR amplification was performed using a thermocycler with the following conditions: initial denaturation at 95°C for 5 minutes, followed by 18 cycles of denaturation at 95°C for 50 seconds, annealing at 55°C for 1 minute, and extension at 68°C for 8 minutes. A final extension step was performed at 68°C for 5 minutes, after which samples were held at 4°C. The expected length of the PCR product was approximately 8kb, and the reaction was allowed to proceed overnight.

The PCR product was verified using agarose gel electrophoresis. A 0.7% agarose gel was prepared in 1X TAE buffer, and 10 µL of 10,000X SYBRSafe DNA stain was added after the agarose was fully dissolved. For analysis, 10 µL of the PCR reaction was mixed with 2 µL of 6X DNA loading dye and loaded onto the gel alongside 5 µL of 1kb DNA ladder (100 ng/µL). The gel was run at 90V for 40 minutes, and the DNA bands were visualized using a UV transilluminator. The remaining PCR reaction underwent DpnI digestion to remove the template plasmid DNA. This was performed by adding 1 µL of DpnI restriction enzyme to the PCR reaction and incubating at 37°C for at least 1 hour.

Bacterial Transformation and Colony Inoculation

Heat shock was transformed by thawing one aliquot (100 µL) of commercial BL21 *E. coli* on ice. The DpnI-digested PCR product (2 µL) was added to the cells and incubated on ice. During this incubation, 500 µL of 1.5X LB media was pre-warmed at 37°C, and the DNA-cell mixture underwent heat shock at 42°C for 90 seconds, followed by a 2-minute ice incubation. The pre-warmed media was added to the mixture and incubated at 37°C with shaking for 1 hour. Following incubation, the transformed cells were pelleted by centrifugation at 13,000 rpm for 1 minute. After removing 400 µL of supernatant, the cell pellet was resuspended in the remaining 100 µL of media. The suspension was spread onto pre-warmed LB-antibiotic plates using sterile colrollers and incubated at 37°C for 16-18 hours. Antibiotic selection was based on the resistance marker of the original template vector (ampicillin for pBB204 or kanamycin for pBB205/pBB206).

Individual transformed colonies were selected for further culture. 5 mL of LB media containing appropriate antibiotics (1X carbenicillin or kanamycin) was prepared for each colony. The antibiotic-containing media was prepared by adding 1X antibiotic (from 1000X stock) to 1X LB media. Single colonies were picked using sterile wooden sticks and inoculated into separate culture tubes containing the selective media. The cultures were incubated at 37°C with shaking for 16-18 hours, with tubes loosely capped to allow proper aeration.

Plasmid DNA Purification

Bacterial cultures were harvested by centrifugation, processing 3 mL of overnight culture in two sequential 1.5 mL aliquots. Each aliquot was centrifuged at 13,000 rpm for 1 minute, with supernatants decanted between spins to collect a single combined cell pellet. Plasmid DNA was purified using the QIAGEN Miniprep Kit. Cell pellets were resuspended in 250 µL Buffer P1 (containing RNase) through gentle pipetting to ensure homogeneous suspension. Cellular lysis was performed by adding 250 µL Buffer P2 and inverting the tubes 4-5 times, followed by a 5-minute room temperature incubation. The lysis reaction was neutralized by adding 350 µL Buffer N3 with 4-6 gentle inversions. Cellular debris was removed by centrifugation at 13,000 rpm for 10 minutes, and the cleared lysate (approximately 850 µL) was carefully transferred to a prepared spin column, avoiding the white residue. The column was processed through a series of centrifugation steps at 13,000 rpm, including a wash with 750 µL Buffer PE. After removing the residual wash buffer through an additional 1-minute centrifugation, plasmid DNA was eluted in 30 µL Buffer EB (10 mM Tris, pH 8.5). DNA concentration was determined using a nanodrop spectrophotometer, with Buffer EB as the blank reference.

DNA Sequencing Preparation

Purified plasmid samples were prepared for sequencing following specific concentration requirements. For each sample, 100-150 ng of plasmid DNA was combined with 1 µL of sequencing primer (3.3 µM) and sterile dH₂O to a final volume of 12 µL. Sequencing primers

were prepared through serial dilutions: PS1 stock primers (100 µM ATGGCGGAGTCTCTGATAAG were first diluted to 10 µM by combining 10 µL of stock with 90 µL sterile dH₂O, followed by a second dilution to 3.3 µM by mixing 10 µL of the 10 µM solution with 20 µL sterile dH₂O.

Transformation into Expression Strain

Stock solutions were prepared before expression experiments. A 1 M benzamide stock was prepared by dissolving 0.174 g benzamide in DMSO to a final volume of 1 mL. A 0.1 M ZnSO₄ solution was prepared by dissolving 28.8 g zinc sulfate in deionized water to a final volume of 1 L.

BL21(DE3) Codon Plus *E. coli* cells were transformed with the pBB204 plasmid using heat shock transformation. Briefly, 1 µL of plasmid DNA was added to 100 µL of competent cells and incubated on ice for 30 minutes. After heat shock at 42°C for 90 seconds and a 2-minute ice incubation, 500 µL of pre-warmed 1.5X LB or SOC media was added. The transformation mixture was incubated at 37°C with shaking for 1 hour. LB-CB-CHL plates containing 10 mM benzamide were prepared by spreading 200 µL of 1 M benzamide on pre-warmed selective plates. The entire transformation mixture was plated and incubated at 37°C for 16-18 hours.

Initial Culture Growth, Expression Culture, and Induction

Single colonies were inoculated into 5 mL LB media containing 0.7X carbenicillin, 0.7X chloramphenicol, and 10 mM benzamide. Cultures were grown overnight at 37°C with shaking for 16-18 hours.

Large-scale expression was performed in 100 mL cultures. The media contained: 1X LB, 0.7X Carbenicillin (70 µL of 1000X stock), 0.7X Chloramphenicol (70 µL of 1000X stock), and 10 mM benzamide (1 mL of 1M stock). Expression cultures were inoculated with 5 mL of overnight culture and grown at 37°C with shaking. Growth was monitored by measuring OD₆₀₀ every hour, using deionized water as the blank. At OD₆₀₀ 0.8-1.0, an uninduced sample (1 mL) was collected by centrifugation at 13,000 rpm for 1 minute and stored at -20°C. Before induction, ZnSO₄ was added to a final concentration of 100 µM (10 µL of 0.1 M stock per 100 mL culture). The culture was chilled on ice for 1 hour, followed by induction with 0.5 mM IPTG (500 µL of 1 M stock). Protein expression was conducted at 25°C with shaking for 16-18 hours.

Cell Harvest and Protein Analysis by SDS-PAGE

Following overnight induction, 1 mL of the induced culture was collected for analysis. Both uninduced and induced 1 mL samples were centrifuged at 13,000 rpm for 1 minute, with supernatants carefully decanted into a 10% bleach solution for decontamination. The remaining ~49 mL of induced culture was transferred to a 50 mL conical tube and centrifuged at 3,500 rpm

for 15 minutes. After decanting the supernatant into bleach solution, the cell pellet was stored at -20°C for subsequent analysis.

Protein expression was analyzed using 8% SDS-PAGE gels. Frozen cell pellets were thawed at room temperature or on a heating block (85°C or above). Cell pellets were resuspended in 100 µL of 5X SDS Loading dye for both uninduced and induced samples. Samples were denatured by boiling for 5 minutes, followed by centrifugation at 13,000 rpm for 1 minute to remove insoluble material. Gel electrophoresis was performed by loading 1 µL of pre-stained protein ladder and 16 µL of each sample. The gel was run at 250V for approximately 30 minutes, or until the loading dye reached the bottom of the gel. Protein visualization was accomplished using AquaStain. For AquaStain visualization, gels were incubated in a pre-used AquaStain solution (usage tracked by tally marks, limited to 5 uses) for 20 minutes with shaking at room temperature. Final destaining was performed in deionized water for 15-20 minutes with shaking.

Results

Our study investigated the cancer-associated PARP1 D229V mutation using a site-directed mutagenesis approach. First, the introduction of the D229V mutation into three PARP1 expression vectors: pBB204 (GST-PARP1), pBB205 (his-flag-mCherry-PARP1), and pBB206 (his-SMT-HA-PARP1) through site-directed mutagenesis, the mutant plasmids purification, DNA sequencing, and protein expression of the mutant plasmid (GST-PARP1 D229V in pGex6-c1) to further investigate the functional consequences of the PARP1 D229V mutation.

The first objective was to introduce the D229V mutation into three different PARP1 expression vectors: pBB204 (GST-PARP1), pBB205 (his-flag-mCherry-PARP1), and pBB206 (his-SMT-HA-PARP1). Following PCR-based mutagenesis, products were analyzed by agarose gel electrophoresis to confirm successful amplification.

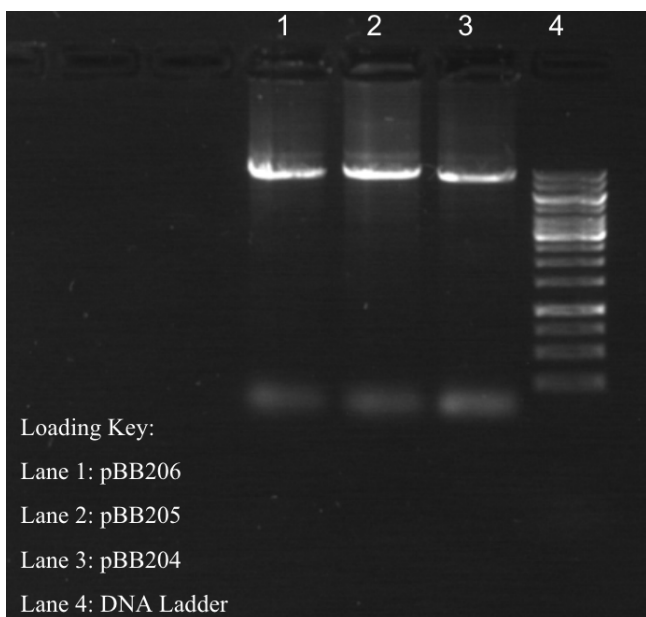
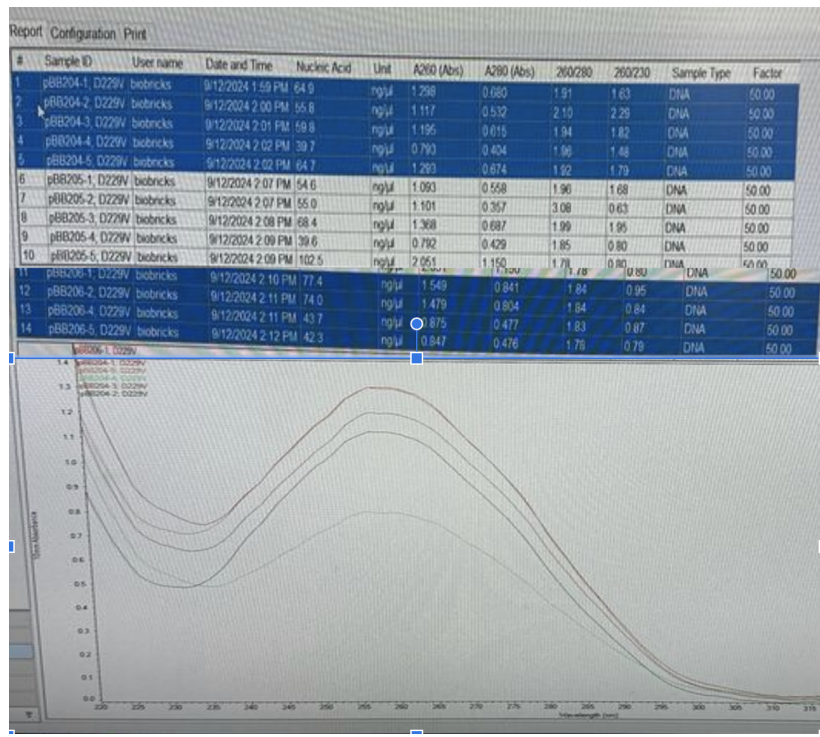


Figure 1: Verification of site-directed mutagenesis PARP1 D229V represented by a 0.7% agarose gel with 1X SYBRsafe, 1kB DNA ladder, and 6X DNA loading dye, ran at 90V for 40 minutes.

The above figure shows an agarose gel (0.7%) electrophoresis of PCR products following site-directed mutagenesis for the D229V PARP1 mutation. PCR products from vectors pBB204, pBB205, and pBB206 show the expected bands. Single, distinct bands indicate successful PCR amplification without non-specific products. After successful PCR verification, the amplified plasmids were purified to remove reaction components and template DNA. The purified plasmid DNA was then quantified using nanodrop spectrophotometry, which measures absorbance at 260nm and provides both concentration and purity ratios (260/280 and 260/230). This quantification step was crucial to ensure sufficient DNA yield and quality.



#1, D229V, pBB204, 64.9 ng/uL
#2, D229V, pBB204, 55.8 ng/uL
#3, D229V, pBB204, 59.8 ng/uL
#4, D229V, pBB204, 39.7 ng/uL
#5, D229V, pBB204, 64.7 ng/uL
#1, D229V, pBB205, 54.6 ng/uL
#2, D229V, pBB205, 55.0 ng/uL
#3, D229V, pBB205, 68.4 ng/uL
#4, D229V, pBB205, 39.6 ng/uL
#5, D229V, pBB205, 102.5 ng/uL
#1, D229V, pBB206, 77.4 ng/uL
#2, D229V, pBB206, 74 ng/uL
#3, D229V, pBB206, -----na-----
#4, D229V, pBB206, 43.7 ng/uL
#5, D229V, pBB206, 42.3 ng/uL

Figure 2: Thermo Fisher Nanodrop Spectrophotometry of Miniprepped D229V in pBB204, pBB205, and pBB206 and the absorbance of each sample at different wavelengths of light.

The measurements revealed pBB204 constructs (n=5): Range 39.7-64.9 ng/ μ L (mean: 56.98 ng/ μ L), pBB205 constructs (n=5): Range 39.6-102.5 ng/ μ L (mean: 64.02 ng/ μ L), and pBB206 constructs (n=4): Range 42.3-77.4 ng/ μ L (mean: 59.35 ng/ μ L). A successful DNA concentration measured by a spectrophotometer is typically between 50 and 100 ng/ μ L, and the quality of the DNA extraction, with a good purity indicated by an A260/A280 ratio between 1.8 and 2.0. These measurements confirm the success of the conducted procedure, with the average of the plasmid constructs being above 50.0 ng/ μ L and 100% of the A260/A280 ratio being over 1.70. The graph demonstrates an ideal absorbance spectrum for pure DNA, showing the characteristic peak at 260 nm with a smooth curve shape. The spectra for all samples display the expected bell-shaped curve with a maximum at 260 nm and minimal absorbance at 230 nm and 280 nm, indicating minimal contamination.

The next experimental objective was to confirm the successful introduction of the D229V mutation through DNA sequencing. Quality metrics were assessed to ensure reliable sequence data.

ID	Sample Name	.seq	.ab1	Primer	QC Value		Length	QV20+
					High Quality	Medium Quality		
					Low Quality			
Note: The QC scores can only give you an overall picture on data quality. For details, please examine the chromatogram of each reaction. (.ab1 column below)								
• QC Value (Trace Score): Average basecall quality value								
• QV20+: The total # of bases in the entire trace that have basecaller quality value \geq 20								
ID	Sample Name	.seq	.ab1	Primer	QC	Length	QV20+	
1	1	1	1	P1	25	527	526	
2	2	1	1	P1	39	861	876	
3	3	1	1	P1	40	930	949	
4	4	1	1	P1	20	179	324	
5	5	1	1	P1	40	606	602	
6	6	1	1	P1	39	914	929	
7	7	1	1	P1	15	4	141	
8	8	1	1	P1	27	763	839	
9	9	1	1	P1	39	906	936	
10	10	1	1	P1	32	580	567	
11	11	1	1	P1	28	892	841	
12	12	1	1	P1	14	14	157	
14	14	1	1	P1	37	905	900	
15	15	1	1	P1	31	463	499	

Figure 3: Quality Assessment of DNA Sequencing Results for PARP1 D229V Mutant Constructs

The figure above displays the sequencing quality metrics for 14 PARP1 D229V mutant samples. High-quality sequences (samples 2, 3, 5, 6, 9, 14) showed read lengths >800 bases and QC values \geq 39, indicating reliable mutation verification. Medium-quality sequences (samples 1, 8, 10, 11, 15) and low-quality sequences (samples 4, 7, 12) required additional verification. These high-quality sequence results indicate a successful D229V mutation introduction probability, while the lower-quality samples may not. Seven out of the fourteen PARP1 D229V mutant samples had high-quality sequences with the successful introduction of the D229V mutation (GAC [ASP] to GTC [VAL] at positions 685-687 bp). The remaining samples had medium or low-quality sequences, most likely due to improper adherence to lab protocol in a step for those seven samples.

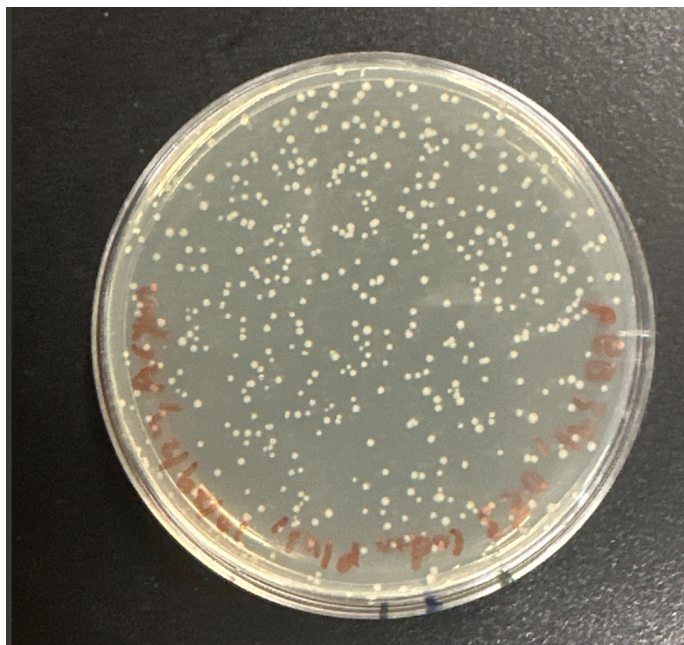


Figure 4: Growth of Transformed Colonies on LB-CB-CHL-benzamide agar plate

Next, the transformation of commercial BL21 *E. coli* with the pBB391 (GST-PARP1 D229V in pGex6-c1) plasmid was successful, as evidenced in Figure 4 by the growth of colonies on the LB-CB-CHL-benzamide agar plate. Following the transformation protocol, a single colony was selected and used to inoculate a 5 mL starter culture in LB-CB-CHL-benzamide-glucose media. The starter culture was then used to sub-inoculate a larger 100 mL culture. The OD₆₀₀ of this culture was monitored, and when it reached the target range of 0.8-1.0, the culture was induced with 100 µM ZnSO₄ and 0.2 mM IPTG. The successful transformation, growth, induction, and harvest of the BL21 *E. coli* expressing the PARP1 D229V mutant construct indicate that the experimental workflow was executed effectively up to this point.

Discussion

Our study has made significant progress in investigating the functional impact of the cancer-associated PARP1 D229V mutation through a molecular biology approach. The successful implementation of site-directed mutagenesis across three distinct expression vectors (pBB204, pBB205, and pBB206) demonstrates the robustness of our approach alongside the flexibility for downstream analyses, which proved valuable given the success rates in the sequencing results. Throughout our experiment, PCR-based mutagenesis succeeded with clear amplification products with single, distinct bands, indicating specific amplification. Including DMSO in the PCR reaction was crucial for successfully amplifying GC-rich regions, representing an important optimization step in our protocol.

DNA quality and yield optimization presented both challenges and opportunities for protocol refinement. Our plasmid DNA yields, averaging between 56.98-64.02 ng/µL across different constructs, consistently stayed within the acceptable range, and the A₂₆₀/A₂₈₀ ratios

exceeding 1.70 indicated high purity. The verification of mutations through sequencing revealed varying quality across samples, with only 7 out of 14 samples showing high-quality sequences confirming the D229V mutation (GAC to GTC). The successful transformation and expression in Commercial BL21 *E. coli* demonstrated the viability of our expression, with the addition of benzamide and careful monitoring of induction conditions for protein stability. Our work provides a robust framework for studying other PARP1 mutations and may lead to refined models of PARP1 regulation in cellular homeostasis.

Enzymatic activity assays comparing wild-type and D229V PARP1 will be essential to understand the functional implications of this mutation. Additionally, studies examining the effects of the D229V mutation on DNA repair capacity, energy metabolism, and cell survival under various damage conditions will be crucial for understanding its role in cancer development. Understanding the impact of the D229V mutation could direct mutation-specific therapeutic approaches and establish a framework for studying cancer-associated PARP1 mutations.

References

1. Ray Chaudhuri, A., Nussenzweig, A. *The multifaceted roles of PARP1 in DNA repair and chromatin remodelling.* Nat Rev Mol Cell Biol 18, 610–621 (2017).
<https://doi.org/10.1038/nrm.2017.53>
2. Fatokun AA, Dawson VL, Dawson TM. *Parthanatos: mitochondrial-linked mechanisms and therapeutic opportunities.* Br J Pharmacol. 2014 Apr;171(8):2000-16. doi: 10.1111/bph.12416. PMID: 24684389; PMCID: PMC3976618.
3. Demény MA, Virág L. *The PARP Enzyme Family and the Hallmarks of Cancer Part 1. Cell Intrinsic Hallmarks.* Cancers. 2021; 13(9):2042. <https://doi.org/10.3390/cancers13092042>
4. Gibson BA, et al. *Chemical genetic discovery of PARP targets reveals a role for PARP-1 in transcription elongation.* Science. 2016; 353(6294):45-50.
5. Langelier MF, et al. *Structural basis for DNA damage-dependent poly(ADP-ribosyl)ation by human PARP-1.* Science. 2012; 336(6082):728-732.